*Thermal Science and Engineering (2022) Volume 5 Issue 2*
doi:10.24294/tse.v5i2.1537

ORIGINAL RESEARCH ARTICLE

# Thermodynamic limits to the productivity of passive solar distillators

**Henry Alberto Salinas-Freire[1*], Osney Pérez-Ones[2], Susana Rodríguez-Muñoz[2]**

[1] *Universidad Técnica de Ambato, Campus Huachi, Av. Los Chasquis y Río Payamino, Ambato, Ecuador. E-mail: ha.salinas@uta.edu.ec*

[2] *Universidad Tecnológica de La Habana José Antonio Echeverría, Ave. 114 N° 11901 e/119 and 127. Marianao, Ciudad Habana, Cuba.*

## ABSTRACT

Seawater desalination has been studied with interest due to the scarcity of fresh water for human consumption. Solar distillation is an old method; the productivity, energy consumption of the process and the cost of the desalinated water thus obtained depend on the efficiency achieved in each of the stages of these systems. The limited capacity to absorb solar radiation and transform it into useful heat for evaporation, interaction with the surrounding medium, and heat losses restricts the overall efficiency of the thermal process and productivity. Since the energy comes from solar radiation, the maximum productivity of this process will be constrained by the magnitude of the total solar radiation available in an area of the planet due to its geographic location, time of year, and local climatic conditions. The processes of this energy will be thermodynamically limited by the heat transfer coefficients achieved in the equipment, the maximum value that the evaporation heat can reach, as long as the losses to the environment by convection and radiation are minimal. Comparative analyses of several proposed models reported data of distillers and reported data of solar radiation that reach average values of up to 7.2–7.4 kwh/m$^2$ in some regions of the planet are presented and estimates are made for the productivity of these equipment that they reach between 6.7 and 6.9 kg/m$^2$ day with a theoretical maximum efficiency of about 0.16 of the total solar radiation.

***Keywords:*** Desalination; Passive Solar Distiller; Solar Distiller Productivity; Solar Distiller Efficiency

**ARTICLE INFO**

Received: 22 September 2022
Accepted: 20 October 2022
Available online: 4 November 2022



## 1. Introduction

Seawater desalination has been known since ancient times[1,2], and it has been reported[1,3,4] that Thales of Miletus and Aristotle mentioned it in their writings and described primitive devices based on boiling water in clay pots or cauldrons and collecting it in sponges on ships would have been used to obtain fresh water during long voyages. Since then, several desalination methods and systems have been studied and developed and have gone from prototypes to large-capacity facilities, which has made it possible to learn about the costs and efficiencies of the stages in each process[5-9].

Among the desalination systems currently in use, those based on renewable energies are being studied with great interest over those that use fossil fuel energy[10-16]. Solar desalination or SD consists of placing seawater in a container where, through a transparent film, generally glass, solar radiation is used to heat the saline solution and evaporate part of the water that passes into the air of the chamber and then condenses when it comes into contact with a colder surface from where it is collected[17,18]. This equipment does not use any other source of energy

and therefore its performance depends on the solar radiation that can be captured, and on the efficiency of the processes inside the equipment.

Due to the way the passive solar desalinators operate, all mass and energy transfer stages have limits, which are analyzed in this work and compared with reported data, in order to determine the maximum theoretical expected productivity.

## 2. Theoretical framework

Passive solar desalinators receive all the energy for their operation from incident solar radiation, which is transferred from the glass cover to the bottom of the distiller and from there, converted into thermal energy to the water, the walls, the bottom and the cover of the equipment. Part of this energy evaporates water and the rest is lost to the environment. Several heat and mass transfer models[19,20], as well as correlations for thermodynamic and transport properties of water and steam[21], are used for their analysis. The mathematical models are used to analyze the behavior of the desalinator under the best operating conditions for water temperature, glass temperature, and solar radiation, and the results are compared. For the development of the present work, a single-shell passive solar still is considered, and represented by the schematic in **Figure 1**.

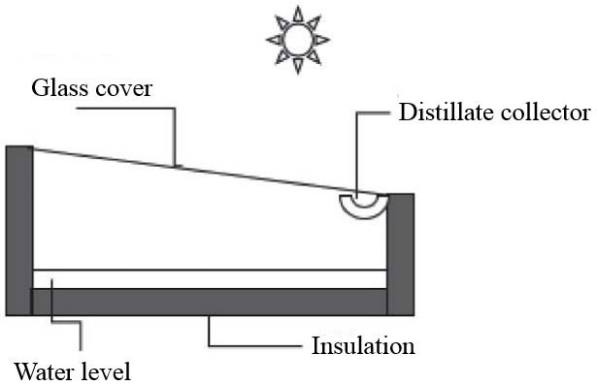


**Figure 1.** Diagram of the passive solar still.

In the distiller, it is considered that there are no mass losses due to equipment leakage, that there are no temperature gradients in the glass, water or insulating material and that the variations due to temperature in the heat capacity of the distiller base of the glass and insulator are negligible[21,22].

## 3. Solar radiation

Solar radiation reaching the earth's surface is not monochromatic[23], which covers a range of wavelengths from the infrared through the visible spectrum to the ultraviolet. In solar desalinators, this radiation $I_b$ reaches the surface of the glass where a small fraction of $\alpha_b$ is absorbed, a small fraction of $\tau_v$ is transmitted and a fraction of $R_v$ is reflected. The transmitted fraction passes through the humid air with negligible losses and reaches the water at the bottom of the still, where again the total radiation is divided between the absorbed $\alpha_w$, reflected $R_wR_w$ and transmitted $\tau_w$. A schematic of this process for glass is shown in **Figure 2**, the transmitted fraction has the same compartment in the air, although with negligible losses, as in the water at the bottom of the distiller.

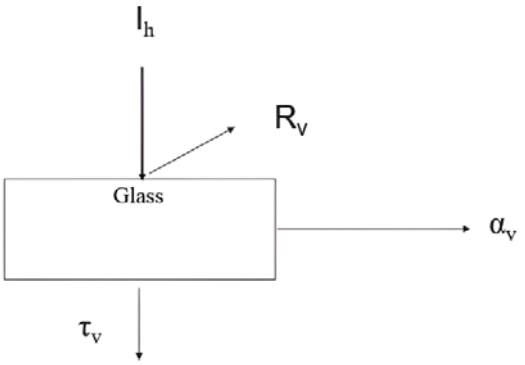


**Figure 2.** Diagram of the process of incidence of solar radiation on glass.

The fraction transmitted by the water reaches the bottom of the distiller, generally painted black, where most of it is absorbed, a small fraction is reflected and practically nothing is transmitted. There it heats the surface of the bottom of the distiller, and this heat begins to be transmitted to the water and to the insulating material on the bottom and walls of the distiller. The water is heated and of the total thermal energy generated that is transferred to the glass, a part is transferred by natural convection, another part by radiation and another part evaporates the water from the saline solution and is transferred in the form of evaporation heat. This is the only fraction of all heat involved in the process that serves to obtain distillate, which transferred to the glass where the vapor is condensed by the temperature difference, and from there it is dissipated by the temperature difference, and from there it is dissipated to the environment[24]. This process is shown in **Figure 3**.

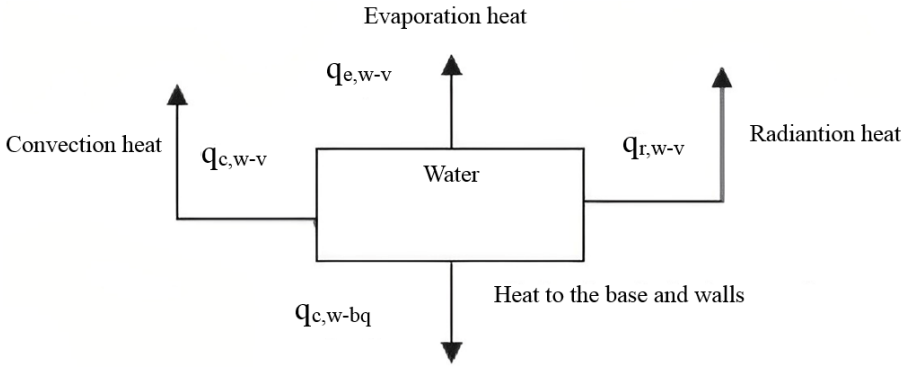


**Figure 3.** Heat transfer from the hot water at the bottom of the distiller.

Solar radiation varies from place to place depending on factors such as geographic location, time of year, cloud cover and time of day. Values can be obtained by direct measurement or through publications from institutions such as the World Bank. Useful data can be found for most regions[25].

In the process of absorption of solar radiation, Cooper[18] and other authors[23] have determined that only 85 to 95% of the incident radiation $I_h I_h$ reaches the bottom of the distiller.

## 3.1 Energy balance

According to the diagram in **Figure 1**, the energy balances are presented as follows[22]:

For the containers with water at the bottom of the distiller:

$$I_h \tau_g \tau_w \alpha_b A_b = h_{c,b-w} A_b (T_b - T_w) + U_f A_f (T_f - T_a) \quad (1)$$

Where:

$I_h = I_h =$ incident radiation on the glass [W/m$^2$],

$\tau_v = \tau_v =$ transmissivity of glass, dimensionless,

$\tau_w = \tau_w =$transmissivity of water, dimensionless,

$\alpha_b = \alpha_b =$absorptivity of the vessel or bottom of the distiller, dimensionless,

$A_b = A_b =$area of the base of the distiller [m$^2$],

$A_f = A_f =$area of the bottom of the distiller [m$^2$],

$h_{c,b-w} =$ convective heat transfer coefficient from the bottom of the distiller to the water [W/m$^2$ °C],

$h_{c,b-w} = T_p = T_p^p =$ distiller bottom temperature [°C],

$T_f = T_f =$ distiller bottom temperature [°C],

$T_w = T_w =$ water temperature [°C],

$U_f = U_f =$ total heat transfer coefficient from the bottom of the distiller to the environment [W/m$^2$ °C], and

$T_a = T_a =$ ambient temperature [°C].

Energy balance for the water in the recipient convection from the bottom of the distiller to the water in the distiller:

$$I_g \tau_g \alpha_p A_w + h_{c,b-w} A_p (T_p - T_w) = m_w c_w \left(\frac{dT_w}{dt}\right) + h_{t,w-v} A_w (T_w - T_{vi}) + U_s A_s (T_w - T_a) \quad (2)$$

Where:

$A_w = A_w =$ area of distiller water [m$^2$],

$m_w = m_w =$ mass of water in the distiller [kg],

$c_w = c_w =$ heat capacity of water [J/kg °C],

$dT_w/dt = dT_w/dt =$ variation of water temperature with respect to time [°C/s],

$h_{t,w-v} = h_{t,w-v} =$ heat transfer coefficient from the water to the glass [W/m$^2$ °C], and

$T_{vi} = T_{vi} =$ temperature of the inner face of the glass [°C].

The total heat transfer coefficient from water to glass, defined by Sampathkumar[26] is:

$$h_{t,w-v} = h_{c,w-v} + h_{r,w-v} + h_{e,w-v} \quad (3)$$

Where:

$h_{c,w-v} = h_{c,w-v} =$ convective heat transfer coefficient of water to glass [W/m$^2$ °C],

$h_{r,w-v} = h_{r,w-v} =$ radiation heat transfer coefficient from water to glass [W/m$^2$ °C],

$h_{e,w-v} = h_{e,w-v} =$ evaporative heat transfer coefficient from water to glass [W/m$^2$ °C].

Energy balance for the roof glass:

$$I_h \alpha_v A_v + h_{t,w-g} A_w (T_w - T_{vi}) =$$

$$h_{r,v-c} A_v (T_{vo} - T_c) + h_{c,v-a} A_v (T_{vo} - T_a) \quad (4)$$

Where:

$\alpha_v = \alpha_v =$ absorbance of the glass, dimensionless,

$A_v = A_v =$ area of the glass [m$^2$],

$h_{rv-c} = h_{rv-c} =$ heat transfer coefficient by radiation from the glass to the sky [W/m$^2$ °C],

$T_{vo} = T_{vo} =$ temperature of the external face of the glass [°C],

$T_c = T_c =$ sky temperature [°C],

$h_{c,v-a} = h_{c,v-a} =$ convective heat transfer coefficient from the glass to the environment [W/m$^2$ °C].

## 3.2 Correlations for water and air properties

To evaluate the coefficients, it is necessary to know the properties of water and air at operating conditions. These properties, such as density, viscosity and vapor saturation pressure, vary as a function of temperature.

**Saturation or vapor pressure of water.** There are several Equations that relate the vapor pressure of water to temperature, of which three are evaluated. The Dunkle correlation[27], valids for temperatures below 70 °C, allows calculation of the vapor pressure P of water in *Pa* at temperature *T* (in °C) and is expressed in Equation 5.

$$P = e^{25.317} - \frac{5144}{T + 273.15} \quad (5)$$

The Antoine Equation[28] also correlates vapor pressures with temperature for substances in a larger range. In the case of water, the Equation that is valid between 0 and 200 °C is:

$$P = e^{23.238} - \frac{3841}{T - 45} \quad (6)$$

Sharma and Mullic[21] present an Equation of Keenan and Keyes (1936) for calculating the vapor pressure of water, which is valid between 10 and 150 °C, by:

$$P = 165960.72 \times 10^{-N} \quad (7)$$

Where:

$$N = \frac{\left[X\left(a + bX + cX^3\right)\right]}{[T(1 + dX)]},$$

X = 647,27 – T,

T = temperature [°C],

a = 3.2437814,

b = 5.86826 × 10$^{-3}$,

c = 1.1702379 × 10$^{-8}$,

d = 2.1878462 × 10$^{-3}$.

**Internal heat transfer.** It includes the energy transferred from the surface of the water to the internal surface of the glass that occurs mainly by radiation, convection and evaporation[26].

**Heat transferred by convection.** The convective heat $q_{c,w-v}$ in W/m$^2$ transferred from the water surface to the glass[29] is defined by Equation 8.

$$q_{c,w-v} = h_{c,w-v} = \left(T_w - T_{vi}\right) \quad (8)$$

Cooper[18], Sharma and Mullick[21] and Sampathkumar[26] establish the heat flux from the water surface to the glass using the Dunkle Equations:

$$q_{c,w-v} = [0.0884(T_w - T_{vi}) + \frac{P_w - P_{vi}}{268.9 \times 10^3 - P_w}](T_w + 273)]^{1/3}(T_w - T_{vi}) \quad (9)$$

According to Sampathkumar[26], the convective heat transfer coefficient can be expressed by:

$$h_{c,w-v} = 0,884\left[\Delta T'\right]^{1/3} \quad (9)$$

$$\Delta T' = \left(T_w - T_g\right) + \frac{\left(P_w - P_{vi}\right)\left(T_w\right)}{\left(268,9 \times 10^3 - P_w\right)} \quad (10)$$

Where

$P_w =$ water vapor pressure at temperature $T_w$, [Pa], and

$P_{vi} =$ vapor pressure of water at glass inner wall temperature, [Pa].

These correlations are valid for operating temperatures around 50 °C and a value of ΔT' around 17 °C, moreover they are independent of the Chamber volume and valid only for heat flow upward in the closed space between the evaporating and condensing surfaces.

**Heat transferred by radiation.** Equation 12 defines the heat transferred by radiation between the water surface and the internal surface of the

glass[29]:

$$q_{r,w-v} = h_{r,w-v}\left(T_w - T_{vi}\right) \tag{11}$$

Where:

$q_{rw-v}$ = heat transferred by radiation, [W/m$^2$]. The radiation heat transfer coefficient is defined in Equation 13 using the Stefan-Woltzman constant σ:

$$h_{r,w-v} = \varepsilon_{ef}\sigma\frac{\left(T_w^4 - T_{vi}^4\right)}{\left(T_w - T_{vi}\right)} \tag{12}$$

Where:

$\varepsilon_{ef}$ = effective emissivity, dimensionless, and $\sigma = 5.67 \times 10^{-8}$ [W/m$^2$ K$^4$].

Cooper[18] and Sharma-Mullick[21] establish an estimated value of 0.9; replacing it in Equation 13 and this in Equation 12 we obtain:

$$q_{r,w-v} = 0{,}9.\ \sigma\left[(T_w)^4 - (T_{vi})^4\right] \tag{13}$$

To obtain more accurate data or particular cases, the effective emissivity is calculated from the emissivities of glass $\varepsilon_v$ and water $\varepsilon_w$, using Equation 15[26].

$$\varepsilon_{ef} = \frac{1}{\frac{1}{\varepsilon_v} + \frac{1}{\varepsilon_w} - 1} \tag{14}$$

**Heat transferred by evaporation.** The heat $q_{e,w-v}$ at W/m$^2$ transferred by evaporation from the water to the glass, as a function of convective heat, according to Cooper[18] is:

$$q_{e,w-v} = 16{,}273\times10^{-3} q_{c,w} - v\frac{\left(P_w - P_{vi}\right)}{\left(T_w - T_{vi}\right)} \tag{15}$$

The values of the coefficients are related according to Setoodeh[30] by Equation 17, where the heat of vaporization of water is assumed to be constant.

$$h_{e,w-v} = 16{,}273\times10^{-3} h_{c,w} - v\frac{\left(P_w - P_{vi}\right)}{\left(T_w - T_{vi}\right)} \tag{16}$$

The evaporative heat transfer coefficient according to Sharma and Mullick[21] is defined by Equation 18. This Equation includes the variations of the heat of vaporization of water with temperature.

$$h_{e,w-v} = \frac{6{,}86\times10^{-9} h_{c,w-v}\left(P_w - P_{vi}\right)h_{fg}}{\left(T_w - T_{vi}\right)} \tag{17}$$

**Total transfer coefficient between water and glass.** According to the balance expressed in Equation 2, the total transfer coefficient can be calculated by Equation 3[26].

**External heat transfer.** Heat is lost in the solar still from the surface of the glass to the environment by natural convection and radiation, and from the walls and bottom of the solar still, which have an insulating material, by radiation and convection[26]. Only the heat lost by the glass to the environment by natural convection and radiation will be analyzed; assuming that in comparison with those, the heat lost by the walls and bottom is negligible.

**Heat transferred by convection.** The convective heat losses $q_{c,v-a}$ in W/m$^2$ of the distiller can be expressed as a function of wind speed. Aboul-Einein[22], Shukla[31] and Sampathkumar[26] use a correlation proposed by Duffie and Beckman (1980) for the heat lost and the transfer coefficient between the glass and the environment:

$$q_{c,v-a} = h_{c,v-a}\left(T_{vo} - T_a\right) \tag{18}$$

$$h_{c,v-a} = 2{,}8 + 3{,}0\mathrm{V} \tag{19}$$

Where:

V = wind speed [m/s].

The convective heat transfer coefficient lost by the solar still from the glass to the atmosphere, or to the sky, according to Sharma and Mullic[21] is defined in Equation 21:

$$h_{c,v-a} = h_w\frac{(T_{vo} - T_a)}{(T_{vo} - T_c)} \tag{20}$$

Where

$h_{c,v-c}$ = convective heat transfer coefficient [W/m$^2$], and

$h_w$ = heat transfer coefficient due to wind [W/m$^2$].

**Radiation heat transfer coefficient between the glass and the environment.** The radiation heat transfer coefficient transferred between the glass and the environment defined by Mullick[21] is:

$$h_{r,v-a} = \varepsilon_v \sigma \, (T_{vo}^2 - T_c^2)\,(T_{vo} - T_c) \quad (21)$$

Where:

$\varepsilon_g$ = glass emissivity, dimensionless

$T_c$ =sky temperature, [K].

**Coefficient of total heat loss between the glass and the environment.** This coefficient comprises the sum of convective and radiative losses, and is expressed by Equation 23:

$$h_{t,g-s} = h_{c,v-c} + h_{r,v-a} h_{t,g-s} = h_{c,v-c} + h_{r,v-a} \quad (22)$$

Where:

$h_{t,g-s}$ = total heat transfer coefficient between the glass and the environment, [W/m$^2$k],

Replacing the definitions of Equation 21 and 22 in Equation 23, we obtain:

$$h_{t,v-c} = h_w \frac{(T_{vo} - T_a)}{(T_{vo} - T_c)} + \varepsilon_v \sigma \, (T_{vo}^2 - T_c^2)\,(T_{vo} - T_c) \quad (23)$$

Some authors[1,27,32] use a correlation shown in Equation 25 to calculate the coefficient of total losses from the glass to the environment as a function of wind speed.

$$h_{t,v-a} = 5{,}7 + 3{,}8V \quad (24)$$

### 3.3 Performance indicators

**Productivity using evaporation heat.** The instantaneous water evaporation rate $\dot{m}_{ew}$ in kg/s, according to Mowla[33], is given by:

$$\dot{m}_{ew} = \frac{q_{ew}}{h_{fg}} \quad (25)$$

The evaporation $M_{ew}$ for a period of time t is:

$$M_{ew} = \int_0^t \dot{m}_{ew} dt \quad (26)$$

If the time period is one hour, in seconds, you have[20,22,31]:

$$m_{ew} = \frac{q_{ew}}{h_{fg}} \times 3600 \quad (27)$$

For Setoodeh[30] and Sampathkumar[26] the mass of evaporated water $m_{ew}$ in a time period $t$ can be calculated by Equation 29.

$$m_{ew} = \frac{q_{ewAw} t}{h_{fg}} \quad (28)$$

Sampathkumar[26] defines daily production, including night hours, as:

$$M_{ew} = \sum_{i=1}^{24} m_{ew} \quad (29)$$

**Productivity using the dimensionless numbers Pr and Gr.** This method[19,26] uses the dimensionless numbers of Prandtl and Grashoff, as shown in Equation 31.

$$h_{e,w-v} = 0{,}016273 \, \frac{k}{d} \, C \, (GrPr)^n \frac{(P_w - P_v)}{(T_w - T_{vi})} \quad (30)$$

Where:

$k$ = thermal conductivity of humid air [W/m °C], and

$d$ = mean characteristic length between evaporating and condensing surfaces [m],

$C$ = constant, dimensionless

$Gr$ = Grashoff number, dimensionless and

$Pr$ = Prandtl number, dimensionless.

The dimensionless Grashoff and Prandtl numbers are:

$$Gr = \frac{\beta g d^2 \rho^2 \Delta T'}{\mu^2} \quad (31)$$

$$\Pr = \frac{\mu C_p}{k} \quad (32)$$

Where:

$\beta$ = factor of the volumetric coefficient of thermal expansion of air [K$^{-1}$],

$\rho$ = vapor density [kg/m$^3$], and

$\mu$ = viscosity of moist air [Pa·s].

Setoodeh[30] also presents a correlation for certain properties that are evaluated at $T_v$ which is the average temperature between $T_w$ and $T_g$:

$$T_v = \frac{T_w + T_g}{2} \quad (33)$$

$$\beta = \frac{1}{(T_v + 273)} \quad (34)$$

$$\rho = \frac{353{,}44}{(T_v + 273{,}15)} \quad (35)$$

$$k = 0{,}0244 + 0{,}7673x10^{-4}T_v \quad (36)$$

Where for T < 70 °C the latent heat of vaporization of water $h_{fg}$ is:

$$h_{fg} = 2{,}4935x10^{6}[1 - 9{,}4779x10^{-4}T_v + 1{,}3132x10^{-7}T_v^2 - 4{,}7974x10^{-9}T_v^3] \quad (37)$$

For viscosity:

$$\mu = 1{,}718x10^{-5} + 4{,}620x10^{-8}T_v \quad (38)$$

The heat capacity of the air:

Replacing the definitions and clearing, it is established[19] that the productivity $m_{ew}$ can be calculated using the Grashoff and Pandtl numbers by means of Equation 41:

$$C_p = 999{,}2 + 0{,}1434T_v + 1{,}101x10^{-4}T_v^2 - 6{,}7581x10^{-8}T_v^3 \quad (39)$$

$$m_{ew} = \frac{0{,}016273}{hfg}\frac{k}{d}\,A_w t\,(P_w - P_g)\,C\,(GrPr)^n \quad (40)$$

The values of C and n are calculated, as proposed by Tiwari[32], by regressions from experimental data; in his work, Sampathkumar[26] states that C and n depend on the specific design of each solar still and the water temperature range in which they operate, so they must be determined in each particular case. Some reported values for C and n are presented in **Table 1**.

**Table 1.** Reported C and n values and their range of validity

| Author | C | N | Validity interval |
|---|---|---|---|
| Kumar and Tiwari[19] | 0.0322 | 0.4110 | $1.794*10^6 < Gr < 5.724*10^6$ |
| Tiwari[32] | 0.0112 | 0.4088 | |
| | 0.0621 | 0.3999 | |
| Sampathkumar[26] | 0.0750 | 0.3300 | $Gr > 3.2*10^5$ |
| Shukla[31] | 0.079–0.065 | 0.329–0.378 | |

**Productivity using incident solar radiation.** P. I. Cooper[18] in his work presents a linear correlation, valid for radiation levels $I_h$ between 0.4 and 1.39 kW/m$^2$ and for an ambient temperature of 30 °C, to calculate the instantaneous productivity which is shown in Equation 42.

$$\dot{m}_{ew} = 3{,}125 * 10^{-4} I_h - 3{,}438{,}10^{-5} \quad (41)$$

### 3.4 Efficiency

**From evaporated water.** To calculate the efficiency $\eta_t$ of a passive solar still from the heat of vaporization, the mass of condensed water and the measured incident radiation, Equation 43[20] is used:

$$\eta_t = \frac{\Sigma m_{ew} h_{fg}}{\left[\Sigma I_{h(t)} A_s\right]\Delta t} \quad (42)$$

Where:

$A_s =$ distiller base area, [m], and

$\Delta t$ = period of time, [s].

**Theoretical maximum efficiency from solar radiation.** Cooper[18] presents an Equation to find the maximum theoretical daily efficiency shown in Equation 45. Using this Equation yields higher data than those found using Equation 44 for the same case.

$$\eta_o = 0{,}727 - 2{,}88\times10^{2}\frac{\theta_s}{I_\tau} \quad (43)$$

Where:

$\eta_o =$ maximum theoretical daily efficiency, dimensionless,

$\theta_s =$ daylight hours of a day measured from sunrise to sunset, [h].

For the calculations, the data[34] of a solar still are considered with the values presented in **Table 2**[22]:

Where $x_a$ and $x_v$ are the thickness of the water and glass, respectively, and $k_v$ is the thermal conductivity of the glass.

**Table 2.** Passive solar still parameters

| | |
|---|---|
| $A_w = 1{,}000m^2 A_w = 1{,}000m^2$ | $R_v = 0{,}05 R_v = 0{,}05$ |
| $A_v = 1{,}035m^2 A_v = 1{,}035m^2$ | $R_w = 0{,}05 R_w = 0{,}05$ |
| $x_a = 0{,}040m\ x_a = 0{,}040m$ | $\varepsilon_w = 0{,}95 \varepsilon_w = 0{,}95$ |
| $x_v = 0{,}004m x_v = 0{,}004m$ | $\varepsilon_v = 0{,}94 \varepsilon_v = 0{,}94$ |
| $d = 0{,}45md = 0{,}45m$ | $a_v = 0{,}05 a_v = 0{,}05$ |
| $k_v = 0{,}0351W/\text{mK} k_v$ | $\theta = 15°\theta = 15°$ |
| $= 0{,}0351W/\text{mK}$ | |

## 4. Results

**Deviations of correlations for estimating water vapor saturation pressure.** The vapor pressure of water between 0 and 100 °C calculated by

the correlations of Antoine, Sharma, and Dunkle differ from each other and from the data of Lemmon, McLinden, and Friend reported in Perry[35]; their deviation is shown in **Figure 4**.

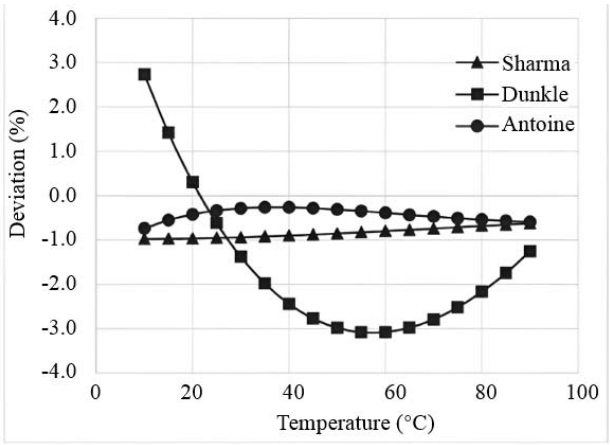


**Figure 4.** Percentage deviation of water vapor pressure calculated according to Dunkle, Antoine and Sharma-Mullick (Keenan-Keyes) correlations.

It can be seen that Dunkle's correlation is the one with the greatest deviations, between +2.7 and -3.1%, while the lowest values are for Antoine's with -0.4 and 0.7%.

## 4.1 Internal heat transfer

### 4.1.1 Convection heat

**Figure 5** shows the behavior of the convective heat transfer coefficient as a function of the water temperature $T_w$ and the temperature of the internal face of the glass $T_{vi}$. It can be seen that it increases as $T_w$ increases and $T_{vi}$ decreases.

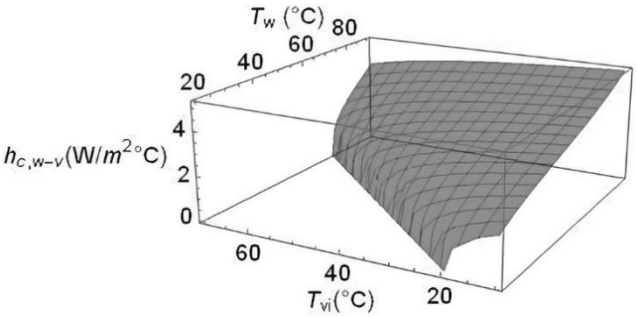


**Figure 5.** Convection heat transport coefficient $h_{c,w-v}$ as a function of water temperature $T_w$ and glass temperature $T_{vi}$.

### 4.1.2 Heat transferred by radiation

The behavior of the radiation heat transfer coefficient with respect to the temperatures of the water $T_w$ and the glass $T_v$ is shown in **Figure 6**. The coefficient can reach 9.0 W/m$^2$ °C when the temperature difference is 50 °C, higher values, when both temperatures are equal or the temperature of the glass is higher than that of the water, are physically meaningless. The magnitude of the coefficient increases as the water temperature increases and the glass temperature decreases.

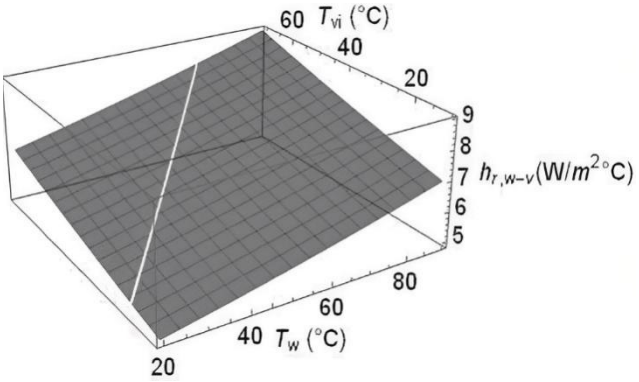


**Figure 6.** Radiative heat transport coefficient $h_{r,w-v}$ as a function of water and glass temperatures.

### 4.1.3 Evaporation heat

The behavior of the evaporative heat transfer coefficient calculated from Equation 17 as a function of water and glass temperatures is shown in **Figure 7**. The value reached by this coefficient is much larger in magnitude than the convective heat and radiant heat, around 120 W/m$^2$ °C for temperature differences of 60 °C, the segment where the glass temperature is higher than the water temperature is physically meaningless.

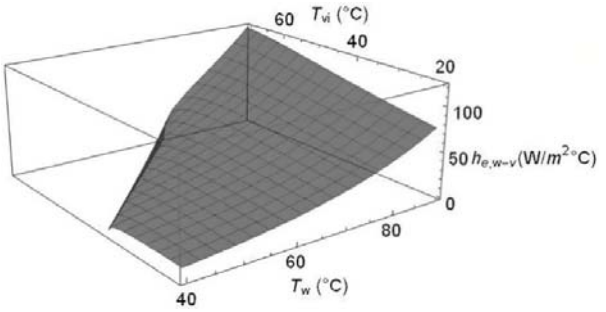


**Figure 7.** Evaporative heat transport coefficient proposed by Mowla and Tiwari $h_{e,w-v}$ as a function of the temperatures of the water $T_w$ and the internal face of the glass $T_{vi}$.

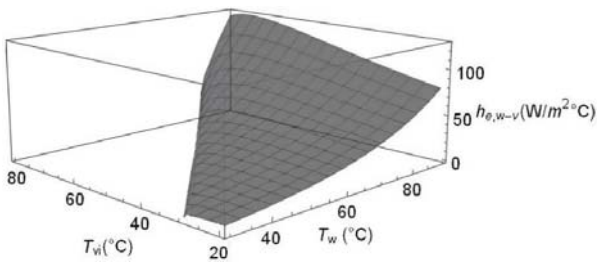


**Figure 8.** Evaporation heat transport coefficient $h_{e,w-g}$ considering the variable heat of vaporization as a function of water and glass temperatures.

The values calculated with Equations 17 and 18 vary little. The behavior of the evaporative heat transfer coefficient between the water and the internal surface of the glass calculated by Equation 18 is shown in **Figure 8**.

### 4.1.4 Total transfer coefficient between water and glass

It corresponds to the sum of heat transferred by radiation, convection and evaporation, is calculated with Equation 3 and is shown in **Figure 9**. This coefficient may reach up to 135 W/m$^2$ °C for temperature differences of 50 °C.

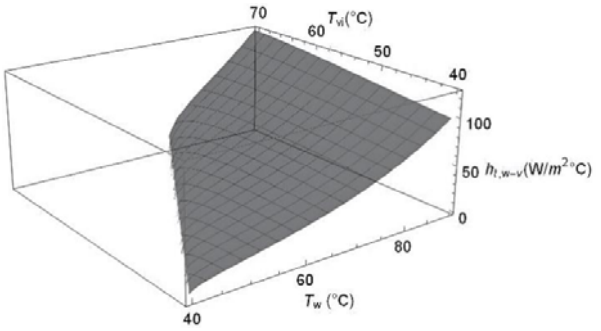


**Figure 9.** Total heat transfer coefficient between water and glass $h_{t,w-v}$ as a function of the temperatures of the water $T_w$ and the internal face of the glass $T_{vi}$.

## 4.2 Performance indicators

### 4.2.1 Productivity using the heat of evaporation

The behavior of the daily productivity calculated from the convective and evaporative transfer coefficients by Equation 30 is shown in **Figure 10** as a function of $T_w$ and $T_{vi}$.

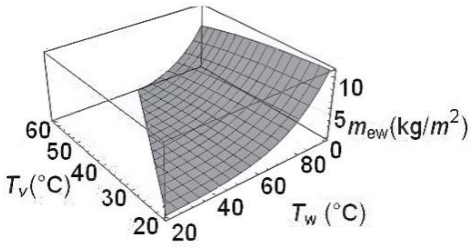


**Figure 10.** Daily distiller productivity calculated using the transfer coefficients, as a function of the water temperatures $T_w$ and the internal face of the glass $T_{vi}$.

### 4.2.2 Productivity using dimensionless numbers

**Figure 11** shows the behavior of productivity as a function of water and glass temperatures, where 0.0112 and 0.4088 have been used for C and n, respectively. It should be noted that in this case, the productivity values are lower than those shown in **Figure 10** at the same temperature conditions calculated using the heat of evaporation. The maximum values reported in practice achieved for productivity are around 0.550 kg/m$^2$h[32]. It can be seen that the productivity increases with the increase of water temperature and decrease of glass temperature.

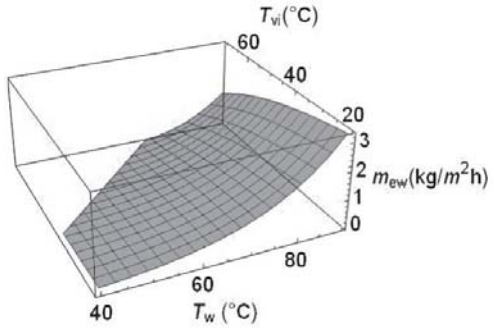


**Figure 11.** Distillate productivity calculated using the dimensionless numbers, as a function of water $T_w$ and glass temperatures $T_{vi}$.

### 4.2.3 Magnitudes of transfer coefficients

Using the transfer models described above, a range of values of heat transfer coefficients can be calculated, which is shown in **Table 3**.

**Table 3** shows that in conditions of low temperatures and low wind speed, the total incident energy can only be used by 37% without considering the losses due to reflection of the transparent material that vary between 10 and 15% of the incident radiation[18], and in conditions of high temperature and high wind speed this evaporative heat can reach up to 62% of the total. This is under ideal conditions, considering for example that all the time the evaporator glass is perpendicular to the incident

**Table 3.** Values reached by heat transfer coefficients in passive solar stills

| | Heat transfer coefficient (W/m$^2$h) | |
|---|---|---|
| | **Minimum** | **Maximum** |
| Internal heat transfer | Tv = 40 °C and Tw = 50 °C | Tv = 50 °C and Tw = 90 °C |
| Convection | 2.61 | 3.98 |
| Radiation | 5.68 | 8.99 |
| By evaporation | 10.56 | 122.20 |
| External heat transfer | Wind speed V = 1 m/s | Wind speed V = 15 m/s |
| Convection losses | 5.8 | 47.8 |
| Total losses | 9.5 | 62.7 |

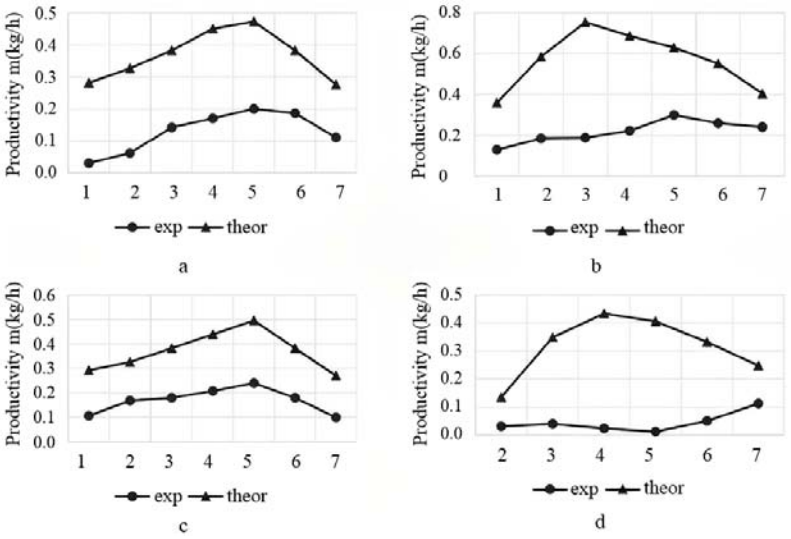


**Figure 12.** Comparison of theoretical and experimental maximum productivities for four cases. **a**) Shukla[31], **b**)[31], **c**)[31] and **d**) Dev[34].

radiation, which is not true for passive solar evaporators. Wind speed affects the process in two ways; by cooling the outer face of the evaporator glass and aiding in condensation, and at the same time cooling the rest of the equipment, so high wind speed increases convection losses.

### 4.2.4 Theoretical and experimental productivities

The theoretical maximum productivity has been calculated from solar radiation using Equation 44 and is shown together with data obtained experimentally in several trials in **Figure 12**.

The theoretical maximum productivities are located between 0.42 and 0.75 kg/h, while the experimental ones reach maximums between 0.15 and 0.30 kg/h. According to the atlas published by the World Bank[25], there are areas of high solar radiation that reach an annual average between 7.2 and 7.4 kW.h/m$^2$, using this model[18], the productivity value of 6.7 to 6.9 kg/m$^2$/day represents a theoretical maximum under ideal conditions.

The theoretical maximum efficiency has been calculated using Equation 43 of the solar radiation model and is presented in **Figure 13,** together with the efficiency obtained experimentally in several tests.

It can be seen that the theoretical maximum efficiency reaches values between 0.25 and 0.63, while the experimental data range between 0.01 and 0.45.

## 5. Conclusions

(1) In a passive solar still, there will ways be convection and radiation transfer mechanisms to the interior, as well as reflection and convection losses to the exterior, therefore the theoretical maximum usable heat to evaporate the water will range between 33% and 56% of the total solar radiation under ideal conditions.

(2) The solar still performance calculated using the heat transfer coefficients model, and that calculated using the dimensionless number correlations provide data that accurately represent the phenomenon, while the correlations based on solar radiation present theoretical maxima for productivity and efficiency, which are consistently higher than those measured in all cases.

(3) The productivity of passive solar stills as a function of available solar irradiation has thermodynamic limits defined for their productivity between 6.7 and 6.9 kg/m$^2$ day, which are determined by the intensity of incident solar radiation, construction materials, local temperature conditions and wind speed.

## Conflict of interest

The authors declare that they have no conflict of interest.

## References

1. Dwivedi VK, Tiwari GN. Experimental validation of

thermal model of a double slope active solar still under natural circulation mode. Desalination 2010; 250(1): 49–55.
2. Hernández H, Rubalcaba E, Hermosillo JJ. Improvement of a MEH desalination unitby means of heat recovery. Energy Procedia 2014; 57: 2781–2786.
3. Moya EZ. Desalinización del agua del mar mediante energías renovables (Spanish) [Desalination of sea water using renewable energies]. Instituto de Estudios Almerienses: Actas del I y II seminario del agua; 1997. p. 199–226.
4. Tiwari GN, Singh HN, Tripathi R. Present status of solar distillation. Solar Energy 2003; 75(5): 367–373.
5. Moore BA, Martinson E, Raviv D. Waste to water: A low energy water distillation method. Desalination 2008; 220(1-3): 502–505.
6. Youssef PG, Al-Dadah RK, Mahmoud SM. Comparative analysis of desalination technologies. Energy Procedia 2014; 61: 2604–2607.
7. Al-Weshahi MA, Tian G, Anderson A. Performance enhancement of MSF desalination by recovering stage heat from distillate water using internal heat exchanger. Energy Procedia 2014; 61: 381–384.
8. Darwish M. Qatar water problem and solar desalination. Desalination and Water Treatment 2014; 52(7-9): 1250–1262.
9. Khayet M. Solar desalination by membrane distillation: Dispersion in energy consumption analysis and water production costs (a review). Desalination 2013; 308: 89–101.
10. Ma Q, Yi C, Lu H, *et al*. A conceptual demonstration and theoretical design of a novel "super-gravity" vacuum flash process for seawater desalination. Desalination 2015; 371: 67–77.
11. El-Sebaii AA, El-Bialy E. Advanced designs of solar desalination systems: A review. Renewable and Sustainable Energy Reviews 2015; 49: 1198–1212.
12. Asiedu-Boateng P, Nyarko BJB, Yamoah S, *et al*. Comparison of the cost of co-production of power and desalinated water from different power cycles. Energy and Power Engineering 2013; 5(1): 26–35.
13. Hamed OA, Kosaka H, Bamardouf KH, *et al*. Concentrating solar power for seawater thermal desalination. Desalination 2016; 396: 70–78.
14. Gabriel KJ, Linke P, El-Halwagi MM. Optimization of multi-effect distillation process using a linear enthalpy model. Desalination 2015; 365: 261–276.
15. Compain P. Solar energy for water desalination. Procedia Engineering 2012; 46: 220–227.
16. Abdelmoez W, Mahmoud MS, *et al*. Water desalination using humidification/dehumidification (HDH) technique powered by solar energy: A detailed review. Desalination and Water Treatment 2014; 52(25-27): 4622–4640.
17. Abdallah SB, Frikha N, Gabsi S. Study of the performances of different configurations of seawater desalination with a solar membrane distillation. Desalination and Water Treatment 2014; 52(13-15): 2362–2371.
18. Cooper PI. The maximum efficiency of single-effect solar stills. Solar Energy 1973; 15(3): 205–217.
19. Kumar S, Tiwari GN. Estimation of convective mass transfer in solar distillation systems. Solar Energy 1996; 57(6): 459–464.
20. Goosen MF, Sablani SS, Shayya WH, *et al*. Thermodynamic and economic considerations in solar desalination. Desalination 2000; 129(1): 63–89.
21. Sharma VB, Mullick SC. Estimation of heat-transfer coefficients, the upward heat flow, and evaporation in a solar still. Journal of Solar Energy Engineering 1991; 113(1): 36–41.
22. Aboul-Enein S, El-Sebaii AA, El-Bialy E. Investigation of a single-basin solar still with deep basins. Renewable Energy 1998; 14(1-4): 299–305.
23. Yeh HM, Ma NT. Energy balances for upward-type, double-effect solar stills. Energy. 1990; 15(12): 1161–1169.
24. Al-Hayeka I, Badran OO. The effect of using different designs of solar stills on water distillation. Desalination 2004; 169(2): 121–127.
25. ESMAP. Global Horizontal Irradiance Poster Map. Solargis; 2017. Available from: www.worldbankgroup.com.
26. Sampathkumar K, Arjunan T, Pitchandi P, *et al*. Active solar distillation—A detailed review. Renewable and Sustainable Energy Reviews 2010; 14(6): 1503–1526.
27. Dunkle RV. Solar water distillation: The roof type still and a multiple effect diffusion still. Proc. International Heat Transfer Conference; 1961 Jan 8-12; University of Colorado, USA. 1961. p. 895.
28. Smith JM, Van Ness HC, Abbott MM. Introduction to thermodynamics in Chemical Engineering. 7th ed. Mexico: Interamericana M-H; 2007.
29. Cengel Y. Heat and mass transfer (a practical approach). 3rd ed. Mexico: McGraw Hill; 2007.
30. Setoodeh N, Rahimi R, Ameri A. Modeling and determination of heat transfer coefficient in a basin solar still using CFD. Desalination 2011; 268(1-3): 103–110.
31. Shukla SK, Sorayan VPS. Thermal modeling of solar stills: An experimental validation. Renewable Energy 2005; 30(5): 683–699.
32. Tiwari GN, Shukla SK, Singh IP. Computer modeling of passive/active solar stills by using inner glass temperature. Desalination 2003; 154(2): 171–185.
33. Mowla D, Karimi G. Mathematical modelling of solar stills in Iran. Solar Energy 1995; 55(5): 389–393.
34. Dev R, Tiwari GN. Characteristic Equation of a passive solar still. Desalination 2009; 245(13): 246–265.
35. Perry RH. Green DW. Perry's Chemical Engineers Handbook. 8th ed. In: Hill M (editor). New York: McGraw Hill; 2008. p. 2735.